APPENDIX II. NOTATIONS

The following symbols are used in this paper:

f = stress;
K = stress relaxation factor for prestressing strands; and
t = time.

Subscripts

pi = initial stress in prestressing steel;
ps = stress in prestressing steel; and
py = yield stress of prestressing steel.

PRESTRESSED COMPOSITE GIRDERS. II: ANALYTICAL STUDY FOR NEGATIVE MOMENT

By Bilal M. Ayyub,[1] Member, ASCE, Young G. Sohn,[2] and Hamid Saadatmanesh,[3] Associate Member, ASCE

ABSTRACT: A method for the structural analysis of prestressed composite steel-concrete girders was studied in this paper. The deflections, forces in the prestressing tendons, and strains in the steel beam and concrete slab of composite girders were computed throughout the entire loading range up to failure. Equations are provided for the calculation of the yield and ultimate load capacities of the girders. The developed analytical models were based on the incremental deformation method. The results of the analytical study were compared with test results of several girders. Reasonably good correlations between analytical and experimental results were obtained. Also, the results showed that a substantial increase in the yield and an increase in the ultimate load capacities can be achieved by adding prestressing tendons to the composite girders and prestressing them. It was determined that the most effective construction sequence for prestressed composite girders in negative moment regions is to posttension the composite girders with tendons in the concrete slabs.

INTRODUCTION

The prestressing of girders in structures introduces initial stresses and strains in directions that are opposite to those induced by external loads. Prestressing composite girders in positive moment regions has long been recognized as an efficient structural system. However, prestressing composite girders in negative moment regions is just starting to receive a general acceptance by the engineering community. In the negative moment region of continuous nonprestressed composite girders, some conservative design practices ignore any contributions of the reinforced concrete slabs of the composite girders and consider only the contributions of the steel beam sections to the structural capacities of the girders. These practices are commonly attributed to the cracked behavior of the concrete slabs. Prestressing composite girders in negative moment regions can prevent cracking of concrete slabs in the service conditions, and reduces the deflection of the girders due to their increased stiffness. Fatigue strength can also be greatly improved by reducing the tensile stress ranges in the top flanges of the girders. The ultimate capacity and the elastic range of the structure can also be increased by adding tendons to the composite girders and prestressing them. Prestressing the critically stressed areas of the girder reduces stresses and deformations, increases the load-carrying capacity, and results in an economical design with efficient use of materials. Providing multiple load paths in the tension region of a girder consisting of the flange and the prestressing

[1]Assoc. Prof., Dept. of Civ. Engrg., Univ. of Maryland, College Park, MD 20742.
[2]Struct. Engr., David Taylor Res. Ctr., Bethesda, MD 20854.
[3]Asst. Prof., Dept. of Civ. Engrg. and Engrg. Mech., Univ. of Arizona, Tucson, AZ 85721.

Note. Discussion open until March 1, 1993. Separate discussions should be submitted for the individual papers in this symposium. To extend the closing date one month, a written request must be filed with the ASCE Manager of Journals. The manuscript for this paper was submitted for review and possible publication on December 18, 1989. This paper is part of the ***Journal of Structural Engineering***, Vol. 118, No. 10, October, 1992. ©ASCE, ISSN 0733-9445/92/0010-2763/$1.00 + $.15 per page. Paper No. 26686.

tendons also adds to structural redundancy, and could reduce the likelihood of catastrophic failure of bridges.

This paper discusses mainly the incremental deformation method for the analysis of prestressed composite steel-concrete girders in the negative moment region. Also, the transformed area method is briefly discussed. The incremental deformation method is used to calculate the stresses and deformations at all levels of loading, including elastic and inelastic regions, up to the ultimate capacity of the girders. The results of the analytical study were compared with test results of several girders.

Previous Work

An early work in this area was by Dischinger (1949), who proposed, in a series of papers, to prestress entire bridges by means of high-strength cables. Szilard (1959) suggested methods for the design of prestressed composite structures. He discussed the analysis for the concrete-steel composite beams based on the assumption of perfect composite action between the slabs and the steel beams. Prestress losses due to creep and shrinkage of concrete and stress relaxation of steel were considered and included in the calculation. Hoadley (1961, 1963) investigated the behavior of simply supported steal beams prestressed with straight high-strength cables and compositely connected to a concrete deck. He developed equations to calculate the stresses and the increase in tendon forces due to applied loads in the elastic region and at the ultimate load. The effects of slip between the slab and steel beam, and of shear connectors on the behavior of conventional composite beams, were experimentally investigated by Viest et al. (1952) and Siess et al. (1952). Various types of shear connectors, mostly channel sections, were investigated by them. It was concluded that the slab reinforcement in the negative moment region was fully effective in contributing to the ultimate moment capacity of the section where shear connectors were provided throughout the region. Similar findings were reported by Culver et al. (1961) and Slutter and Driscoll (1962). Regan (1966) studied analytically the behavior of single-span prestressed composite beams. The effects of varying the prestressing force and tendon size on the load capacity of the beams were investigated and compared with the corresponding effects of the variation of cover plate sizes for conventional composite beams. The subcommittee on prestressed steel of the joint ASCE-AASHO committee on steel flexural members reviewed the state of knowledge in the area of prestressed steel girders in 1968 (Ekberg 1968). The committee summarized three methods to analyze prestressed flexural members, and provided a comparison between prestressed girders and conventional nonprestressed girders. Tochacek and Amrhein (1971) discussed the concept of allowable stresses and factors of safety as applied to prestressed steel structures.

Saadatmanesh et al. (1989a) studied the behavior of prestressed composite beams and developed analytical prediction models. They compared the analytical results with experimental data of a prestressed composite beam that was tested by the same researchers. (Saadatmanesh et al. 1989b). However, their first test was limited to a composite beam made of a rolled steel section. Basu et al. (1987) studied experimentally and analytically the behavior of two-span partially prestressed composite beams to verify the analytical predictions on the basis of experimental data. They concluded that partial prestressing increased the capacity of the girders by about 20%. They also concluded that prestressing effectively prevented slab cracking and

stiffness loss in negative moment regions under service conditions. The cracks that would occur due to overloads were observed to close upon unloading. Dunker et al. (1986) studied posttensioning distribution in composite bridges, and Dunker et al. (1988 and 1990) studied posttensioning methods for strengthening three-span continuous bridges. They conducted model and field tests, and compared the results to predicted structural responses based on finite element analyses. The concepts of prestressed steel structures were also studied by Tochacek (1971), Troitsky et al. (1989), and Troitsky (1990).

The techniques of prestressing composite girders have been developed not only for strengthening existing bridges,but for new bridge construction. For example, these techniques were recently used, as described by Seim et al. (1982), for the new construction of the Bonner's Ferry bridge in northern Idaho. The steel plate girders used in this bridge have spans ranging from 30.5 m (100 ft) to 47.2 m (155 ft). The bridge was prestressed only in the negative moment regions using two stages for prestressing. In the first stage, the steel plate girders were prestressed before concrete placement of the slabs. Consequently, this prestressing force reduced the tensile stresses of the relatively thin top flange due to the weight of the slabs. Then, the composite concrete-steel girders were prestressed, in the second stage, by tendons in the concrete slabs. Therefore, the entire span of the bridge was designed to be in full composite action under service loads. Transverse prestressing was also used in this bridge. The writers discussed several benefits for prestressing, including weight and cost reductions, vertical deflection reduction, and higher redundancy by providing multiple load paths.

Analytical Method

The incremental deformation method was mainly used in this paper for the analysis of prestressed composite girders in negative moment regions. The following assumptions were made in the analysis for a typical cross section of a prestressed composite plate girder in a negative moment region, as shown in Fig. 1:

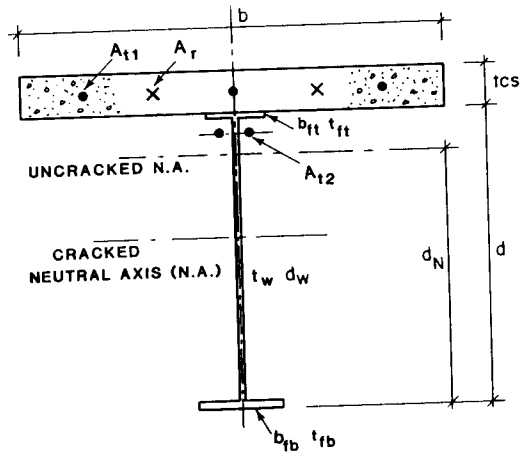

FIG. 1. Typical Cross Section of Girder at Negative Moment Location

1. For the steel beams and prestressing tendons, the elastoplastic relationship, as shown in Fig. 2(*a*), was assumed. For the concrete in the slabs, the stress-strain relationship, as shown in Fig. 2(*b*), was assumed. The concrete in tension was assumed to perform linearly, whereas in compression it was modeled using a higher-order polynomial.
2. The strain distribution across the full depth of the composite girder was assumed to be linear.
3. Deformations caused by concrete creep and shrinkage are not considered. However, relaxation of the prestressing tendons was considered. (Ayyub et al. 1990).
4. Residual stresses in the steel plate girders were not considered.
5. Perfect composite action was assumed. In the analysis, no slip or shear-stud deformation was assumed.
6. The assumptions of beam theory and small angles were used.
7. The prestressing tendons were assumed to be longitudinally restrained

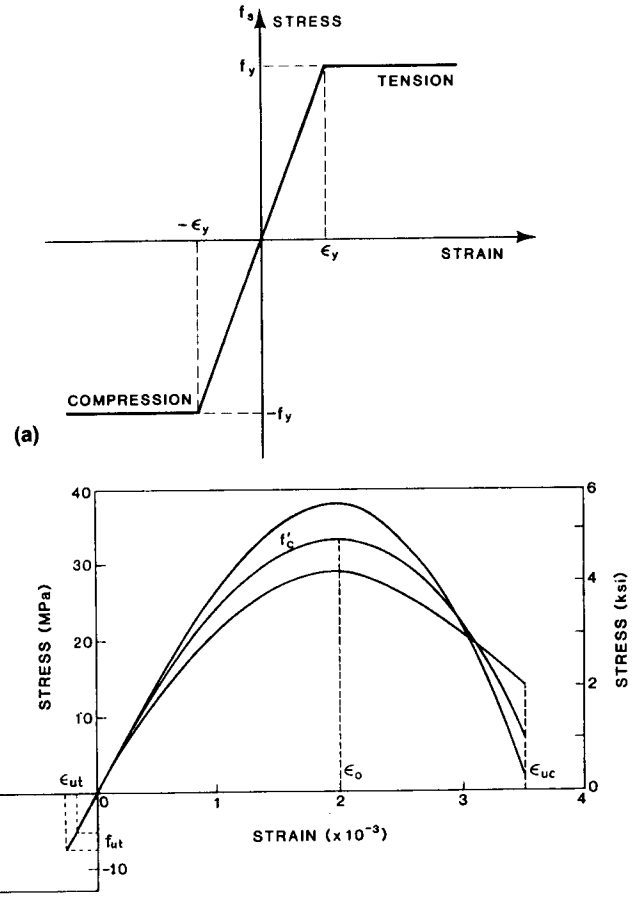

FIG. 2. Stress-Strain Relationships: (*a*) Idealized Stress-Strain Relationship for Steel; (*b*) Idealized Stress-Strain Relationship for Concrete

at their ends and positioned at a constant distance from the plate girders throughout the loading range.

Construction Sequences

Construction and prestressing sequences are very important in determining the stresses in the concrete, steel girders, and tendons of prestressed composite girders. The analysis and design of a prestressed composite girder could change significantly, depending on the sequence of construction and prestressing. The following three construction sequences were identified in this study:

1. Construction sequence (a): According to this construction sequence, the concrete slab of a composite section should be fabricated as a precast pretensioned element. The steel plate girder should be prestressed separately, and then it is compositely connected to the concrete slab by grouting special pockets in the slab that are provided at the shear-stud clusters (or groups) on the top flange of the girder.
2. Construction sequence (b): The concrete slab in this sequence should be fabricated as a precast pretensioned element, and then it is compositely connected to the steel plate girder by grouting the pockets in the slab around the clusters of the shear connectors. Then, the composite girder should be posttensioned either by tendons in the concrete slab or by tendons under the top flange of the steel girder.
3. Construction sequence (c): The composite girder is firstly constructed without any prestressing. The concrete slab in this case can be a cast-in-place element. Then, the composite girder is posttensioned either by tendons in the concrete slab or by tendons under the top flange of the steel girder.

Construction sequences (a) and (c) were recently investigated by Ayyub et al. (1990) by structurally testing five girders that were constructed according to the two sequences. Therefore, the discussed method of analysis in this paper was applied to these two construction sequences for the purpose of illustration. In analyzing or designing prestressed composite girders according to these sequences of construction, two stages of loading should be considered, an initial stage where the stress effects of the the prestressing force and dead load are considered, and a final (service) stage where the stress effects of live load, impact load, and the loads of the initial stage are considered.

Construction Sequence (a)

In the initial stage, the stress in the concrete slab due to a prestressing force applied at midthickness of the slab is given by

$$f_c = -\frac{T_{ic}}{A_{cs}} \quad \ldots\ldots (1)$$

The prestressing-induced stress in the steel girder is given by

$$f_s = -\frac{T_{is}}{A_s} - \frac{T_{is} e_s y}{I_s} \quad \ldots\ldots (2)$$

where T_{ic} = initial force in prestressing tendons in concrete slabs; A_{cs} = cross-sectional area of concrete slab; A_s = cross-sectional area of steel girder;

T_{is} = initial force in prestressing tendon for steel girder; I_s = moment of inertia of steel girder; e_s = eccentricity of tendons in steel girder measured from the centroid of the steel girder, positive below the centroid and negative above the centroid; and y = distance from the centroid of steel girder to any point in the cross section, positive above the centroid and negative below the centroid. At this stage, the dead load of the concrete slab and steel girder (CL) is carried only by the steel girder. The stress in the steel girder due to dead load is given by

$$f_s = -\frac{\Delta T_{DL}}{A_s} + \frac{M_{DL} - \Delta T_{DL} e_s}{I_s} y \quad \ldots\ldots (3)$$

where M_{DL} = magnitude of dead load moment; and ΔT_{DL} = increase in tendon force due to dead load, given by Hoadley (1963) as

$$\Delta T_{DL} = \frac{\frac{e_s}{L}\int_0^L M_{DL}\, dx}{e_s^2 + \frac{E_s I_s}{E_t A_t} + \frac{I_s}{A_s}} \quad \ldots\ldots (4)$$

where L = span of girder; dx = length differential along centroidal axis of girder; A_t = cross-sectional area of tendon; and E_s and E_t = moduli of elasticity of steel girder and tendon, respectively.

In the final stage, the transformed cross section of the composite girder carries the live and impact load (LL). The stress in the concrete slab due to this load is given by

$$f_c = \frac{\alpha}{n}\left(-\frac{\Delta T_{LL}}{A_{tr}} + \frac{M_{LL} - \Delta T_{LL} e_{tr}}{I_{tr}} y_{tr}\right) \quad \ldots\ldots (5)$$

The stress in the steel girder is given by

$$f_s = -\frac{\Delta T_{LL}}{A_{tr}} + \frac{M_{LL} - \Delta T_{LL} e_{tr}}{I_{tr}} y_{tr} \quad \ldots\ldots (6)$$

where A_{tr} = area of transformed composite section; I_{tr} = moment of inertia of transformed composite sectoin; y_{tr} = distance from centroid of composite section to any point in cross section, positive above centroid and negative below centroid; e_{tr} = eccentricity of prestressing tendon from centroid of transformed composite section, positive below centroid and negative above centroid; ΔT_{LL} = increase in tendon force due to live and impact load; M_{LL} = magnitude of live and impact load moment; n = the modular ratio E_s/E_c; E_c = elastic modulus of concrete; and α = 1 for uncracked slab and 0 for fully cracked slab. The increase in tendon force due to live and impact load can be computed using an equation that is similar to (4) and based on transformed section properties.

The stresses in the plate girder due to prestressing, as given by (2), should be checked for any possible instabilities of its components as required by design specifications [e.g., *Standard* (1983)]. The stresses due to dead, live, and impact loads, as given by (3)–(6), act in opposite directions to prestressing stresses at corresponding locations. Therefore the prestressing of composite girders has the benefit of increasing the elastic as well as the stable range of the plate girders.

Construction Sequence (c)

Before applying any prestressing force and with the concrete slab cast, the initial stage stress in the steel girder due to dead load of slab is given by

$$f_s = \frac{M_{DL}}{I_s} y \quad \ldots\ldots (7)$$

In this case, the composite section is assumed to be posttensioned, with tendons in the concrete slab. Therefore, the stress in the steel girder is given by

$$f_s = -\frac{T_{ic}}{A_{tr}} - \frac{T_{ic} e_{tr}}{I_{tr}} y_{tr} \quad \ldots\ldots (8)$$

The stress in the concrete slab is given by

$$f_c = \frac{\alpha}{n}\left(-\frac{T_{ic}}{A_{tr}} - \frac{T_{ic} e_{tr}}{I_{tr}} y_{tr}\right) \quad \ldots\ldots (9)$$

In the final stage, the stress in the steel girder and concrete slab due to live and impact load (LL) can be similarly determined as follows:

$$f_s = -\frac{\Delta T_{LL}}{A_{tr}} + \frac{M_{LL} - \Delta T_{LL} e_{tr}}{I_{tr}} y_{tr} \quad \ldots\ldots (10)$$

$$f_c = \frac{\alpha}{n}\left(-\frac{\Delta T_{LL}}{A_{tr}} + \frac{M_{LL} - \Delta T_{LL} e_{tr}}{I_{tr}} y_{tr}\right) \quad \ldots\ldots (11)$$

The increase in the tendon force due to LL can be determined using a similar approach as given by (4). The stresses at the top of the concrete slab (f_{tcs}), and the extreme fibers of top (f_{tf}) and bottom (f_{bf}) steel flanges due to live and impact load (LL) are respectively given by

$$f_{tcs} = \frac{\alpha}{n}\left[-\frac{\Delta T_{LL}}{A_{tr}} + \frac{-\Delta T_{LL} e_{tr}(d + t_{cs} - d_N) + M_{LL}(d + t_{cs} - d_N)}{I_{tr}}\right] \quad \ldots\ldots (12)$$

$$f_{tf} = -\frac{\Delta T_{LL}}{A_{tr}} + \frac{-\Delta T_{LL} e_{tr}(d - d_N) + M_{LL}(d - d_N)}{I_{tr}} \quad \ldots\ldots (13)$$

$$f_{bf} = -\frac{\Delta T_{LL}}{A_{tr}} + \frac{-\Delta T_{LL} e_{tr} d_N + M_{LL} d_N}{I_{tr}} \quad \ldots\ldots (14)$$

where d = depth of steel girder; t_{cs} = thickness of concrete slab; and d_N = distance from centroid axis of composite girder to exterior surface of bottom steel flange. Other parameters were previously defined. Once the top surface of the concrete slab reaches the allowable tensile stress, i.e., modulus of rupture, A_{tr}, e_{tr}, d_N, and I_{tr} should be recalculated according to the cracked section, in which the concrete slab is excluded from calculations of section properties. The final computational step is to add up the stresses of the initial stage [as given by (7), (8), and (9)] to the stresses due to live and impact load [(10) and (11)] in order to determine the total stresses in

the final stage. The total stresses are then compared with the corresponding allowable stresses outlined in relevant design specifications.

Incremental Deformation Method

The incremental deformation method computes strains, stresses, deformations, and forces based on numerically satisfying the conditions of force equilibrium and deformation compatibility for prestressed composite girders at any loading level. The method can be used for predicting the structural response of girders in the elastic as well as inelastic ranges of loading. According to this approach, the strain in the extreme fiber of a prestressed composite girder is assumed to increase in specified increments. The strains at all levels of interest within the cross section of the girder are then calculated using an assumed linear stress diagram, i.e., using similar triangles. The resulting strains are expressed in terms of the unknown location of the neutral axis. The corresponding stresses are then calculated from the stress-strain relationshps for the corresponding materials. At each strain level, the location of the neutral axis is iteratively calculated based on satisfying the condition of force equilibrium using a numerical method, e.g., bisection method. The internal resisting moment is then calculated by summing up the bending moments of the section forces with respect to the neutral axis. The applied load is then calculated using an equation that relates the internal moment at the investigated cross section to external moment at the same section due to external loads. The resulting strains are then used to determine the curvature variation along the span of the beam, which is needed to compute the deformations of interest. The details of these computational steps are described in the remaining part of this section.

Stress-Strain Relations

The stress-strain curves for the concrete and the steel of plate girders and tendons were assumed as shown in Fig. 1.

Strains

The strains at all levels across the depth of the cross section are determined based on the assumed strain (ε_{s1}) at the bottom steel flange and the unknown

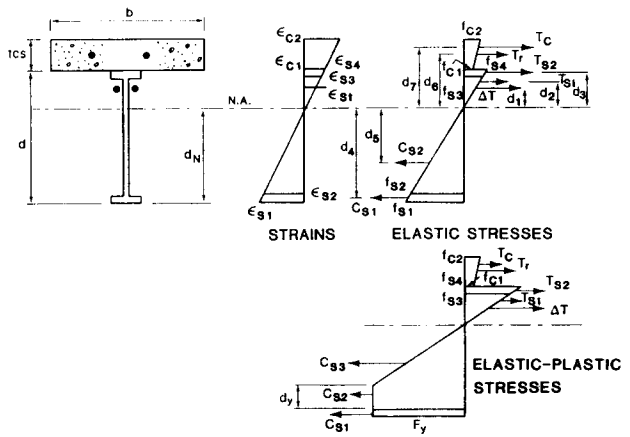

FIG. 3. Stress and Strain Distribution across Girder Depth

location of the neutral axis (d_N). As shown in the strain diagram of Fig. 3, the strains are calculated from similar triangles in the strain diagram. The following relations are accordingly obtained:

$$\varepsilon_{s1} = -\varepsilon_{s1} \quad \ldots\ldots (15a)$$

$$\varepsilon_{s2} = \frac{d_N - t_{bf}}{d_N}\varepsilon_{s1} \quad \ldots\ldots (15b)$$

$$\varepsilon_{s3} = \frac{d - d_N - t_{tf}}{d_N}\varepsilon_{s1} \quad \ldots\ldots (15c)$$

$$\varepsilon_{s4} = -\frac{d - d_N}{d_N}\varepsilon_{s1} \quad \ldots\ldots (15d)$$

$$\varepsilon_{c1} = \alpha\varepsilon_{s4} \quad \ldots\ldots (15e)$$

$$\varepsilon_r = -\frac{d + 0.5t_{cs} - d_N}{d_N}\varepsilon_{s1} \quad \ldots\ldots (15f)$$

$$\varepsilon_{c2} = -\frac{d + t_{cs} - d_N}{d_N}\varepsilon_{s1} \quad \ldots\ldots (15g)$$

$$\varepsilon_t = \frac{\Delta T}{A_t E_t} \quad \ldots\ldots (15h)$$

where t_{bf} = thickness of bottom steel flange; t_{tf} = thickness of top steel flange; ε_{s1} = assumed strain at bottom surface of bottom flange, which is increased in specified increments; ε_{s1}, ε_{s2}, ε_{s3}, and ε_{s4} = strains in the steel beam, as shown in Fig. 3; ε_{c1} and ε_{c2} = strains in the concrete; ε_t = strain in tendon; and ε_r = strain in the reinforcing bars in the concrete slab. Other parameters in (15) were previously defined.

Stresses

The stress diagrams for the elastic and elastoplastic regions are shown in Fig. 3 for a composite cross section under a negative moment. The stresses at all levels across the depth of the girder are calculated from the stress-strain relationships of the materials using the computed expressions of the corresponding strains. The stress-strain relationships can be linear or nonlinear.

Internal Forces

The internal forces in the cross section are determined by integrating the stresses over the corresponding areas of action. A general internal force equation is given by

$$\mathcal{F}_i = \int_{\text{overstress area } \mathcal{A}} f_i \, d\mathcal{A} \quad \ldots\ldots (16)$$

where f_i = stress; $\mathcal{A}$ = coresponding stress area; and $\mathcal{F}_i$ = force that can be either tension (T) or compression (C), as shown in Fig. 3.

Location of Neutral Axis and Internal Resisting Moment

The location of the neutral axis d_N can be determined based on the equation of force equilibrium across the depth of the cross section as follows:

$$\Delta T + \sum_{\text{all forces}} \mathcal{F}_i = 0 \quad \ldots\ldots (17)$$

where ΔT = increase in tendon force due to application of external loads. Eq. (17) can be solved iteratively for the value of d_N that satisfies the force equilibrium condition.

The internal resisting moment is then calculated by summing up the bending moments of internal forces with respect to the neutral axis using the following equation:

$$M = \Delta T d_1 + \sum_{\text{all forces}} \mathcal{F}_i d_i \quad \ldots\ldots (18)$$

where d_i = moment arms, as shown in Fig. 3.

External Loads

The external loads that result in the computed internal moment can be determined from equating the internal resisting moment to the external moment due to the applied loads.

Tendon Force Increase due to External Loads

The prestressed composite girder can be considered as an internally indeterminate structure to the first degree. The increase in tendon force due to external loads can be determined based on a deformation compatibility condition, which requires the elongation of the tendon due to tendon force increase (ΔT) to be equal to the girder elongation at the level of the tendon between the anchorage points of the tendon due to external loads.

In the elastic region of the materials, the bending moment, strain at tendon level ε, and curvature ϕ diagrams due to, for example, a concentrated load at midspan are shown in Fig. 4 with the length fraction $a = 0$. The external load and bending moments, in this case, are less than the corresponding yield values. The elongation of the tendon δ_t due to its force increase ΔT is given by

$$\delta_t = \frac{\Delta T L}{A_t E_t} \quad \ldots\ldots (19)$$

The deformation of the steel girder at the tendon level (δ_s) is determined by integrating the strains at that level between the anchorage points of the tendon. For the beam shown in Fig. 4, this deformation is equal to the area under the strain diagram. The strain ε_a in the girder ends at the tendon level is caused by the increase in the tendon force and is given by

$$\varepsilon_a = \frac{\Delta T e^2}{EI} \quad \ldots\ldots (20)$$

The increase in the tendon force ΔT can now be calculated from equating δ_t and δ_s. The resulting tendon force increase is given by

$$\Delta T = \frac{\varepsilon_s}{\dfrac{2}{A_t E_t} + \dfrac{e^2}{EI}} \quad \ldots\ldots (21)$$

where ε_s = strain at tendon level.

The inelastic behavior of a girder begins by exceeding the elastic limit of one or more of the materials. In this case, the elastic-plastic strains should

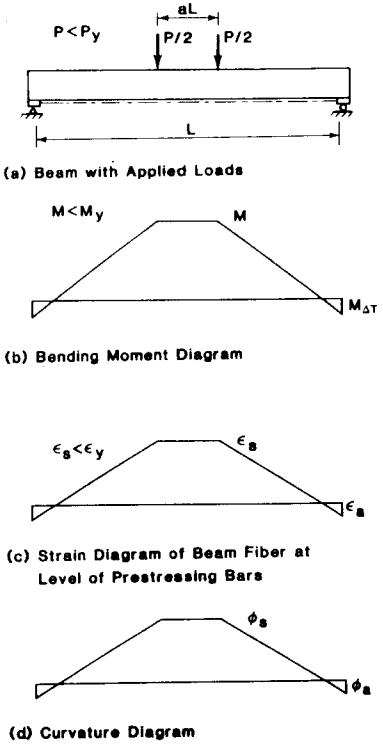

FIG. 4. Moment, Strain, and Curvature Diagrams in Elastic Range

be considered as shown in Fig. 5, with $a = 0$. In this figure, the bending moment, strain at steel level ε, and curvature ϕ diagrams due to, for example, a concentrated load at midspan are shown. The increase in the tendon force ΔT can be similarly calculated from equating δ_t and δ_s. These deformations can be calculated using (19) and the area under the strain diagram in Fig. 5, respectively. The resulting tendon force increase is given by

$$\Delta T = \frac{A_t E_t}{L}\left[(L - L_e)(\varepsilon_y + \varepsilon_a) + \frac{1}{2}(L - 2L_e)(\varepsilon_s - \varepsilon_y) - \varepsilon_a L\right] \quad \ldots\ldots (22)$$

where $L_e = [L(M_{\Delta T} + M_y)/[2(M_{\max} + M_{\Delta T})]$, which is the length of the elastic region as shown in Fig. 5; M_y = first-yield moment of the section; $M_{\Delta T}$ = moment due to tendon force increase that can be computed as $(\Delta T e)$; and $M_{\max}$ = maximum moment due to external loads, which is greater than the yield moment and less than the ultimate moment of the section. A value for the maximum moment should be assumed in order to determine the length L_e, then the assumed value for the maximum moment should be compared with the resulting internal moment, as given by (18). An iterative computational method is needed to determine the necessary condition for having the two moments equal in magnitude. This approach should be combined with the iterations for calculating the location of the neutral axis in nested double-iteration loops.

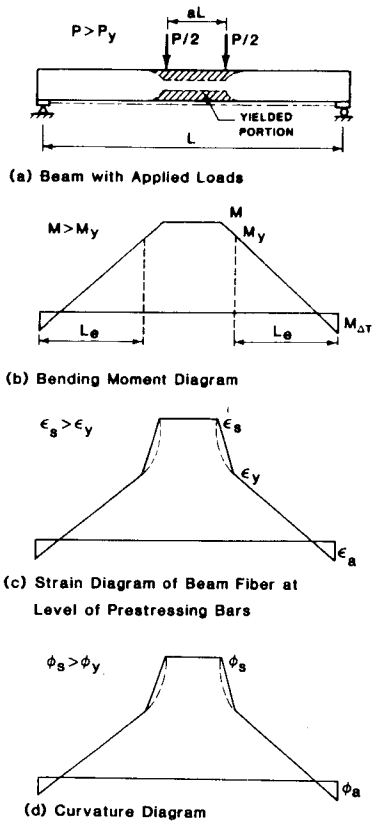

FIG. 5. Moment, Strain, and Curvature Diagrams in Elastic-Plastic Range

Deformations

The deformations of the girder are calculated at the final stage of analysis after determining the location of the neutral axis and strains across the depth of the girder. The deformations are determined based on the curvature diagram as shown in Figs. 4 and 5, where the curvature ϕ_s at midspan of the girder is determined by dividing the strain ε_s by its distance to the neutral axis and the curvature ϕ_a is determined as follows:

$$\phi_a = \frac{M_{\Delta T}}{EI} \quad \ldots\ldots (23)$$

Therefore deformation computations can be based on these curvature diagrams using any appropriate method, e.g., the moment area method. The incremental deformation method of analysis accounts for only flexural deformations, which are the major contributor to deformation. Shear deformation can significantly contribute to the resulting deformations, especially for deep girders. The inclusion of shear deformations in the analysis requires the use of energy methods. For all practical design purposes, shear deformations can be neglected, particularly for relatively large girder-span-to-depth ratios. In this study, shear deformations were not considered.

Ultimate Strength Analysis

The ultimate strength of a prestressed composite section is dependent upon its geometry, the strength properties of steel girders, and prestressing tendons strength. The concrete is assumed to be fully cracked when the ultimate moment capacity of the section is reached. Fig. 6 shows the stress distribution at the ultimate strength of a prestressed composite girder. The girder's cross section should be designed efficiently so that the prestressing tendons always act in tension throughout the entire range of loading. The forces at ultimate capacity can be determined as follows, and are shown in Fig. 6:

$$T_{t1} = A_{t1}F_{yt} \quad \text{for tendon in slab} \quad \ldots\ldots (24a)$$

$$T_{t2} = A_{t2}F_{yt} \quad \text{for tendon in girder} \quad \ldots\ldots (24b)$$

$$T_r = A_rF_{yr} \quad \text{for reinforcing bars} \quad \ldots\ldots (24c)$$

$$T_c = 0 \quad \text{for concrete slab} \quad \ldots\ldots (24d)$$

$$T_{s1} = b_{tf}t_{tf}F_y \quad \text{for top steel flange} \quad \ldots\ldots (24e)$$

$$T_{s2} = t_w(d - d_N - t_{tf})F_y \quad \text{for steel web in tension} \quad \ldots\ldots (24f)$$

$$C_{s2} = t_w(d_N - t_{bf})F_y \quad \text{for steel web in compression} \quad \ldots\ldots (24g)$$

$$C_{s3} = b_{bf}t_{bf}F_y \quad \text{for bottom steel flange} \quad \ldots\ldots (24h)$$

where T = tension force; C = compression force; F_y = yield stress of steel girder; F_{yt} = yield stress of prestressing tendons; F_{yr} = yield stress of reinforcing bar; A_{t1} = total cross-sectional area of tendons in concrete slab; A_{t2} = total area of tendons in steel girder; A_r = total area of reinforcing bars; b_{tf} and b_{bf} = widths of top and bottom flanges of steel girder, respectively; t_{tf} and t_{bf} = thickness of top and bottom flanges, respectively; t_w = thickness of the web; d_N = location of neutral axis measured from extreme fibers of bottom flange; and d = depth of steel girder. If the neutral axis would move above the prestressing tendons as the applied load approaches the ultimate load, the tendons would lose their prestressing forces

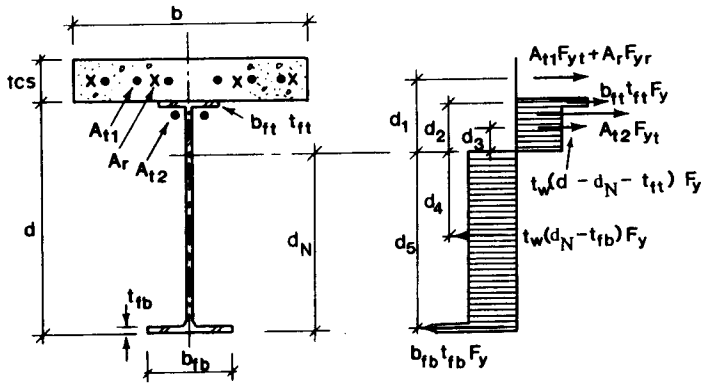

FIG. 6. Ultimate Stress Distribution

and become ineffective in providing additional strength. The location of the neutral axis d_N is given by

$$d_N = \frac{1}{2t_w F_y}(A_{t1}F_{yt} + A_r F_{yr} + A_{t2}F_{yt} + b_{tf}t_{tf}F_y - b_{bf}t_{bf}F_y) + \frac{1}{2}(d - t_{tf} + t_{bf}) \quad \ldots\ldots (25)$$

The moment arms measured from the neutral axis are calculated from the geometry of the cross section and are shown in Fig. 6. The ultimate moment capacity M_u is given by

$$M_u = (A_{t1}F_{yt} + A_r F_{yr})d_1 + b_{tf}t_{tf}F_y d_2 + t_w(d - d_N - t_{tf})F_y d_3 + t_w(d_N - b_{bf})F_y d_4 + b_{bf}t_{bf}F_y d_5 \quad \ldots\ldots (26)$$

Comparison of Analytical Results with Experimental Data

Ayyub et al. (1990) tested experimentally five composite girders that were designed, constructed, and prestressed according to construction sequences (a) and (c) as previously described. These girders were designated as girders A, B, C, D, and E. Girders A, B, C, and D were built according to construction sequence (a). Girder E was built according to construction sequence (c) and posttensioned by tendons in the concrete slab. The cross

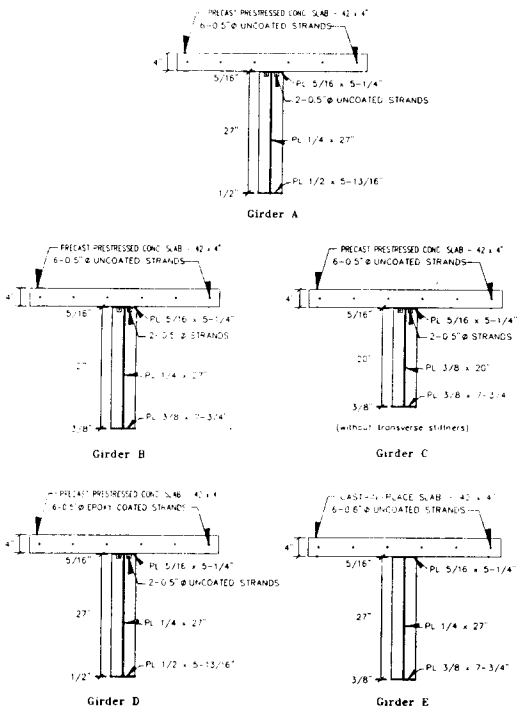

FIG. 7. Cross-Sections of Girders at Midspan (1 in. = 25.4 mm; 1 ft = 304.8 mm)

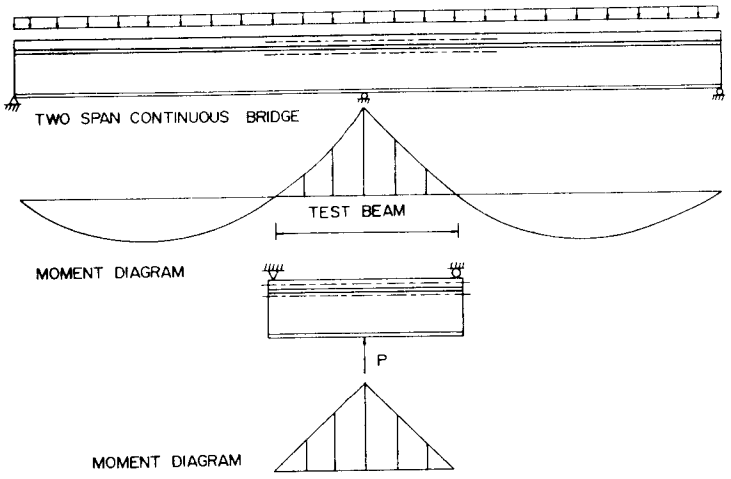

FIG. 8. Simulation of Negative Moment Region

sections of thse girders are shown in Fig. 7. To approximately simulate the negative moment region of a two-span continuous girder, the specimens were tested as upsidedown simply supported with one concentrated load applied at midspan, such that the concrete was subjected to increasing tensile stresses, as shown in Fig. 8. The overall span of the girders was 4.57 m (15 ft). The prestressing tendons in the steel girders were positioned 25.4 mm (1.0 in.) from the extreme fiber of the tension flange of steel girders. The prestressing tendons in the concrete slabs were positioned at its midthickness. The details of these girders, structural tests, and results were provided by Ayyub et al. (1990). Details of the girders are summarized in Tables 1 and 2 of the companion paper. Fig. 9 shows the experimental stress-strain characteristics of the steels used for the plate girders reinforcing bars in the concrete slabs, and prestressing strands. The ultimate strength of the slab's concrete in compression for girders A, B, C, D, and E were 24.8 MPa (3.60 ksi), 36.2 MPa (5.26 ksi), 37.9 MPa (5.50 ksi), 34.9 MPa (5.06 ksi), and 35.9 MPa (5.20 ksi), respectively. The ultimate strength of the slab concrete in tension for girders A, B, C, D, and E were 2.4 MPa (0.35 ksi), 3.3 MPa (0.47 ksi), 2.9 MPa (0.42 ksi), 3.3 MPa (0.47 ksi), and 3.3 MPa (0.47 ksi), respectively. The steel girders has a total of 40 16-mm-diameter (5/8-in.) shear studs grouped in clusters of four at a spacing of 508 mm (20 in.) between the group centers. Shear-stud pockets of the size 127 × 152 mm (5 × 6 in.) were provided in the precast pretensioned concrete slabs for the purpose of grouting the shear studs to achieve composite action between the steel girders and concrete slabs. Bearing stiffeners were provided at the ends and midspan of the girders, and stiffeners were provided at intermediate points at about 660-mm (26-in.) spacing starting from midspan. Girder A was laterally supported at the ends of the simple span, whereas girders B, C, D, and E were laterally supported at the ends, quarter points, and midspan, according to AASHTO specifications (*Standard* 1983). The complete details of these girders, tests setup, and results were provided by Ayyub et al. (1990).

The load-versus-deflection curves for the five girders are shown in Fig. 10. The solid curves represent the experimental data and the nonsolid curves

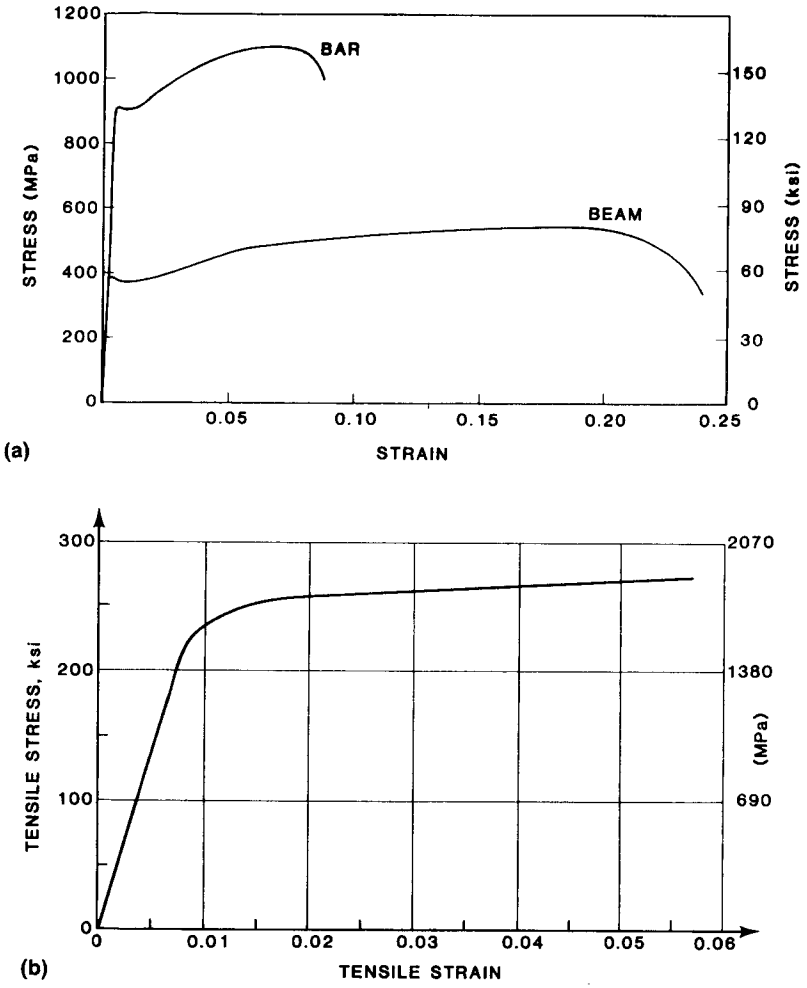

FIG. 9. Experimental Stress-Strain Characteristics of Steels: (*a*) Reinforcing Bars and Plate Girders; (*b*) Prestressing Strands

show the analytical results. The analytical curves consist of two segments that correspond to before and after cracking of the concrete slab. The analytical curves were based on flexural deformations. The experimental curves are well contained between the analytical curves that correspond to the uncracked and cracked concrete sections. The analytical models assume an abrupt transition from uncracked section behavior to fully cracked section behavior, whereas in real structures the transition is gradual, as indicated by the test results.

Comparison of test results of girders B and E showed similar performance for the two specimens. They reached the same ultimate load, which is equal to the calculated yield load, as shown in Fig. 10. The number of prestressing tendons in the concrete slab was the same for girders B and E. However, girder E did not have any prestressing tendons in the steel girder. Since the

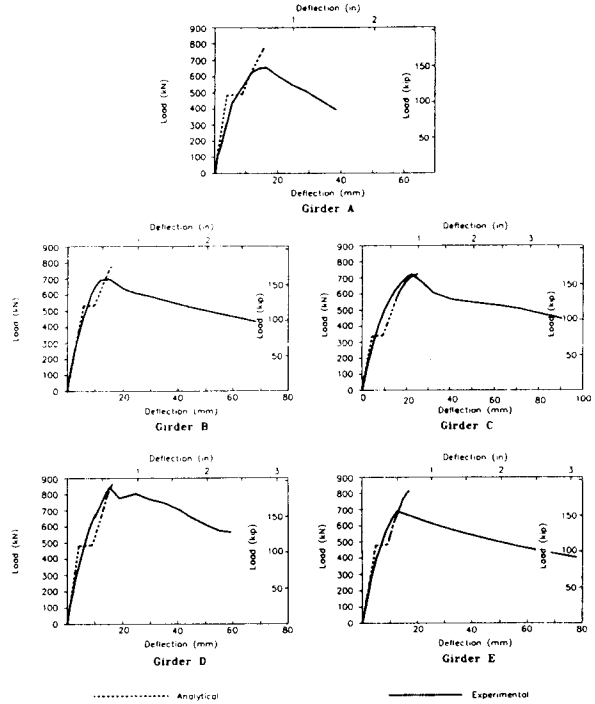

FIG. 10. Load-Deflection Behavior

total cross-sectional area of prestressing tendons in girder E was smaller than those in girder B, it was concluded that construction sequence (c), which was used for girder E, was the most effective sequence. On the other hand, the prestressed precast concrete slabs for the composite girders might have better quality than the cast-in-place slabs. Moreover, an expected reduction in structural construction cost and time and an enhancement of concrete strength and durability are potential benefits of using precast elements.

If, on the other hand, instead of providing prestressing tendons in the concrete slabs, they are provided in the steel girder as per construction sequence (c), the structural performance would not have been as effective as that of girder E. This conclusion was shown experimentally and analytically by Saadatmanesh et al. (1989).

Structural Instability

Lateral-torsional buckling and local buckling are the main factors affecting the ultimate (maximum) strength of the prestressed composite girders in negative moment regions. Girder A was not laterally supported, and therefore failed prematurely due to lateral-torsional buckling. Girder B, C, D, and E were laterally supported according to AASHTO specifications (*Standard* 1983). These specimens failed due to local buckling. The lateral bracing system prevented effectively the lateral-torsional buckling. The maximum resisting loads of the specimens agreed reasonably well with the corresponding analytical yield loads as summarized in Table 1. In this table, the pre-

TABLE 1. Yield and Ultimate Loads of Girders

Girder (1)	Experimental maximum load kN (kips) (2)	Analytical		
		Cracking load kN (kips) (3)	Yield load kN (kips) (4)	Ultimate load kN (kips) (5)
A	670 (151)	490 (110)	730 (164)	936 (210)
B	712 (160)	535 (120)	720 (162)	936 (210)
C	735 (165)	340 (76)	560 (126)	736 (165)
D	860 (193)	592 (133)	725 (163)	936 (210)
E	700 (157)	590 (133)	700 (157)	955 (215)

dicted yield loads correspond to the first yield of any component of the cross sections of the girders, whereas the ultimate loads were based on reaching the full plastic condition of stresses, as shown in Fig. 6. The stresses due to the prestressing forces were added to the stresses due to the applied loads in the analytical model. Girders B and E, which have noncompact webs and compression flanges, had good agreement between their maximum resisting loads and the corresponding analytical yield loads. Therefore the analytical buckling load for a prestressed girder is larger than that for a girder without prestressing, due to the pretension in the compression flange. As a result, prestressing composite girders increased the buckling load capacity of the girders. Girder D consisted of a noncompact web and a compact flange. The maximum resisting load of the girder D was above the analytical yield load due to its postbuckling strength resulting from a tension field action. Therefore, for the same cross-sectional area of a compression flange plate, it is recommended to provide a thicker flange with a smaller width, i.e., a compact section.

Summary and Conclusions

The incremental deformation method of analysis was developed for prestressed composite steel-concrete girders in negative moment regions. The results of the analytical method were compared with experimental test results (Ayyub et al. 1990) to assess the accuracy of the analytical method. The following conclusions are drawn based on the test data and analyses:

The analytical models based on the incremental deformation method agreed reasonably well with the structural behavior of tested specimens in the elastic range.

The analytical model based on the incremental deformation method adequately predicted the structural behavior of the tested specimens in the elastic and inelastic ranges.

The first-yield capacities of the studied girders agreed reasonably well with the corresponding measured maximum (buckling) capacities of the specimens tested by Ayyub et al. (1990). Therefore, the tensile stresses in the bottom flange at the support helped increase the local buckling load of the web and flange of the steel girder, and helped increase the overall strength of the composite beam.

For the same cross-sectional area of a compression flange plate, it is recommended to provide a thicker flange with a smaller width, i.e., a compact section. The girder with the compact compression flange has an additional capacity due to a postbuckling strength.

The prestressing tendons should be placed as far as possible from the centroidal axis in order to have less prestressing force and more tension stresses in the bottom flange of the steel girder as a result of prestressing. To achieve the most favorable stress distribution for composite sections in negative moment regions, the composite sections should be posttensioned by means of tendons in the concrete slabs.

Acknowledgment

The writers would like to acknowledge the financial support of the National Science Foundation (grants ECE-8413204 and ECE-8513648). Any findings, opinions, conclusions, and recommendations expressed in this paper are those of the writers and do not necessarily reflect the views of the National Science Foundation. The help of Jaykant Parekh in preparing this manuscript is also acknowledged.

Appendix I. References

Ayyub, B. M., Sohn, Y. G., and Saadatmanesh, H. (1990). "Prestressed composite girders: experimental study for negative moment." *J. Struct. Engrg.*, ASCE, 118(10), 2743–2762.

Ayyub, B. M., Sohn, Y. G., and Saadatmanesh, H. (1990). "Prestressed composite girders under positive moments." *J. Struct. Engrg.*, ASCE, 116(11), 2931–2951.

Basu, P. K., Sharif, A. M., and Ahmed, H. U. (1987). "Partially prestressed continuous composite beams I and II." *J. Struct. Engrg.*, ASCE, 113(9), 1926–1938.

Culver, C., Zarzeczmu, P. J., and Driscoll, G. C. (1961). "Test of composite beams for buildings." *Report No. 279.6*, Progress Report 2, Fritz Engineering Laboratory, Lehigh University, Bethlehem, Pa.

Dischinger, F. (1949). "Stahlbrucken im verbundmit stahlebeton druckplatten bei gleichzeitiger vorspannung durch hochwertige seite." *Der Bavingerniever*, 24(11), 321–332 (in German).

Dunker, K. F., Klaiber, F. W., and Sanders, W. W., Jr., (1988). "Post-tensioned strengthening of a three-span continuous bridge." *Bridge research in progress proceedings*, Bridge Engineering Center, Iowa State University, Ames, Iowa.

Dunker, K. F., Klaiber, F. W. and Sanders, W. W., Jr. (1986). "Post-tensioning distribution in composite girders." *J. Struct. Engrg.*, ASCE, 112(11), 2540–2553.

Dunker, K. F., Klaiber, F. W., Daoud, F. K., and Sanders, W. W., Jr. (1990). "Strengthening continuous composite bridges." *J. Struct. Engrg.*, ASCE, 116(9), 2464–2480.

Ekberg, C. E. (1968). "Development and use of prestressed steel flexural members." *J. Struct. Engrg.*, ASCE, 94(9), 2033–2060.

Hoadley, P. G. (1961). "An analytical study of the behavior of prestressed steel beams," Ph.D. thesis, University of Illinois, Urbana, Ill.

Hoadley, P. G. (1963). "Behavior of prestressed composite steel beams." *J. Struct. Div.*, ASCE, 89(3), 21–34.

Regan, R. S. (1966). "An analytical study of the behavior of prestressed composite beams," Ph.D. thesis, Rice University, Houston, Tex.

Saadatmanesh, H., Albrecht, P., and Ayyrub, B. M. (1989a). "Analytical study of prestressed composite beams." *J. Struct. Engrg.*, ASCE, 115(9), 2364–2381.

Saadatmanesh, H., Albrecht, P., and Ayyub, B. M. (1989b). "Experimental study of prestressed composite beams." *J. Struct. Engrg.*, ASCE, 115(9), 2349–2364.

Seim, C. H., Herr, L., and Lin, T. Y. (1982). "Cable-stressed steel bridges." Committee on Steel Design, Transportation Research Board, Washington, D.C.

Seiss, C. P., Viest, I. M., and Newmark, N. M. (1952). "Studies of slab and beam highway bridges: part III." *Bull. series no. 396*, Engineering Experimental Station, University of Illinois, Urbana, Ill.
Slutter, R. G., and Driscoll, G. C., Jr. (1962). "Test results and design recommendations for composite beams in buildings." *Report n. 279.10*, Progress Report 3, Fritz Engineering Laboratory, Lehigh University, Bethlehem, Pa.
Standard specifications for highway bridges. 13th Ed. (1983). The American Association of State Highway and Transportation Officials, Washington, D.C.
Szilard, R. (1959). "Design of prestressed composite steel structures." *J. Struct. Div.*, ASCE, 85(9), 97–123.
Tochacek, M., and Amrheim, F. G. (1971). "Which design concept for prestressed steel." *AISC Engrg. J.*, 8(1), 18–30.
Troitsky, M. S. (1990). *Prestressed steel bridges*. Van Nostrand Reinhold Company, New York, N.Y.
Troitsky, M. S., Zielinski, Z., and Rabbani, N. (1989). "Prestressed-steel continuous span girders," *J. Struct. Engrg.*, ASCE, 115(5), 1357–1370.
Viest, I. M., Siess, C. P., Appleton, M. H., and Newmark, N. M. (1952). "Full scale tests on channel shear connectors and composite T-beams," *Bull. Series 405*, Engineering Experimental Station, University of Illinois, Urbana, Ill.

Appendix II. Notation

The following symbols are used in this paper:

A = cross-sectional area;
a = fraction of girder length;
b = width;
C = compressive force;
d = depth of girder or distance;
dx = integral differential along span;
$d\mathcal{A}$ = integral differential for stress action area;
E = modulus of elasticity;
e = eccentricity;
F = tensile strength;
f = stress at any point;
f' = ultimate compressive strength;
I = moment of inertia;
L = span of girder or length;
M = moment;
n = modular ratio;
P = external force;
T = tension force;
t = thickness;
y = distance from centroid or neutral axis of steel girder to point in cross section;
$\mathcal{A}$ = cross action area;
δ = elongation;
ΔT = increase in tendon force;
α = 1 for uncracked concrete slab and 0 for fully cracked concrete slab;
ε = strain at any point;
ϕ = curvature; and
$\mathcal{F}$ = force.

Subscripts

a = end anchorage;
bf = bottom steel flange;

c = concrete;
cs = concrete slab;
DL = Dead load;
e = elastic;
i = dummy variable;
ic = initial in concrete slab;
is = initial in steel girder;
LL = live and impact load;
N = neutral axis;
r = reinforcing bars;
s = steel plate girder;
$s1$ = a component of cross-section of steel girder;
$s2$ = a component of cross-section of steel girder;
$s3$ = a component of cross-section of steel girder;
t = tendon;
$t1$ = prestressing tendons in concrete slab;
$t2$ = prestressing tendons in steel girder;
tcs = top of concrete slab;
tf = top steel flange;
tr = transformed section;
u = ultimate;
uc = ultimate compression;
ut = ultimate tension;
y = yield; and
w = web.